WWW.IJRPR.COM

International Journal of Research Publication and Reviews

Journal homepage: www.ijrpr.com ISSN 2582-7421

Sensor Fusion for Incipient Hydrogen Detection Using Deep Learning

Milad Hadizadeh Masali [1], Reza Barzegaran [2],Hassan Zargarzadeh [3]

[1,2,3]- Phillip M. Drayer Electrical Engineering Department, Lamar University, Beaumont, TX, USA
mhadizadehma@lamar.edu[1], barzegaran@gmail.com[2], hzargarzadeh@lamar.edu[3]
Doi : https://doi.org/10.55248/gengpi.5.0924.2419

ABSTRACT

As a result of the ongoing fluctuations in the global climate, there has been a persistent increase in the necessity of renewable energy sources. Hydrogen has the potential to play a crucial role as an energy carrier during the transition away from fossil fuels. To ensure safe operations, it becomes imperative to possess a dependable and sensitive system for detecting hydrogen leaks. Nonetheless, relying solely on a singular sensor may prove inadequate for detecting minor alterations or abrupt peaks. Sensor fusion systems, which combine data from several sensors, can improve hydrogen gas detection capabilities. This study proposes a real-time AI-based sensor fusion scheme for multi-sensor hydrogen leak detection that incorporates electromagnetic, ultrasonic, and optical sensors. This ensures a combination of reliability and speed that can't be reached using each of these sensors solely.

Keywords: hydrogen, hydrogen detection, leak detection, electromagnetic sensor, ultrasonic sensor, optical sensor, deep learning, LSTM.

1. Introduction

Hydrogen is a versatile and clean energy carrier with potential in transportation, electricity generation, and industrial processes [1]. However, it is highly hazardous if not handled properly [2]. Despite promising applications of hydrogen detection systems, there are challenges due to their flammability and the expanding availability of storage and transportation methods [3-5]. Proactively mitigating hydrogen leakage is crucial to fully realize the advantages of this eco-friendly fuel source [6] using cost-effective reliable, accurate, and fast [7-8]. In the field of hydrogen gas leak detection, several prevalent technologies exist, the most widely used sensors are electrochemical sensors [9] and optical sensors [10]. Electrochemical sensors, even though susceptible to cross-sensitivity with other gases, demonstrate a sufficient level of sensitivity in hydrogen gas detection, ultimately resulting in imprecise alerts. Moreover, they require regular calibration and maintenance to preserve consistent accuracy and reliability [11]. On the other hand, optical sensors offer exceptional precision and selectivity, albeit at an elevated cost and a more intricate implementation process. Additionally, environmental variables such as temperature and humidity can significantly influence the effectiveness of optical sensors [12]. To overcome the single monitoring systems, sensor fusion techniques can be utilized to enhance the detection performance and reliability [13]. By integrating different types of sensors, the system becomes more sensitive to changes or anomalies in the environment, allowing it to recognize subtle or unexpected events more effectively. This integration also helps reduce false alarms by cross-referencing data from multiple sensors to validate the presence of a real threat or anomaly, saving time and resources by avoiding unnecessary responses [14]. Additionally, sensor fusion enables a more comprehensive analysis of environmental factors, such as temperature and humidity, providing a richer and more reliable picture of the situation and making the detection approach more robust and adaptable to different conditions. There are several sensor fusion methods available, each with its own advantages and disadvantages. One common method is Kalman filtering, widely used in applications such as navigation and robotics [15]. Particle filtering, on the other hand, is a more versatile technique capable of handling non-linear and non-Gaussian systems. It proves particularly useful in complex or highly dynamic environments. [16]. Another sensor fusion approach is sensor-level fusion, where raw data from various sensors are directly combined. This method offers fine-grained control over the fusion process and can be valuable in scenarios where leveraging each sensor's unique characteristics is essential [17]. Recent research has concentrated on enhancing the identification and measurement of gas leaks through the utilization of sensor fusion methods. These approaches aim to increase the sensitivity and accuracy of detecting gases that are colorless, odorless, and tasteless, which are challenging for human senses to perceive, by merging data from various sensors such as gas sensors and thermal cameras [18]. The integration of artificial intelligence and multimodal sensors aids in reducing false alarms, improving sensitivity, and providing a comprehensive analysis of environmental factors. Nevertheless, there are limitations associated with lighting conditions, sensitivity to air humidity, and the complexities involved in image processing. Another track of investigation focuses on quantifying gas leakage in biogas plants, achieved by employing a combination of optical sensors, thermal cameras, and sensors based on tunable diode laser absorption spectroscopy (TDLAS) [19-20]. This technique offers the benefit of quantifying gas emissions, providing remote sensing capabilities, and enhancing safety. However, there are challenges such as the requirement for temperature variations for gas cameras to detect greenhouse gas emissions, cross-sensitivity issues with gas cameras, and limitations in the detection of specific gases using active sensors like TDLAS. Long short-term memory (LSTM) is a critical element in this project, which plays a key role in improving the sensor fusion hydrogen gas detection performance. LSTM uses the past to model time-series gas concentration data and

identify anomalies, thereby enhancing safety measures and early warning [21-22]. In effect, LSTM utilizes "gates", which are neurons that employ a sigmoid activation function and are multiplied with the output of other neurons. The LSTM can selectively disregard specific inputs by utilizing gates and preserves a collection of values that are safeguarded by the gates and are not subjected to an activation function [23]. LSTM is utilized to optimize processing and learning, minimize storage needs, and expedite information transfer, ultimately improving the system's efficiency and practicality also suitable for deployment in real-time systems. The proposed scheme in this work is able to distinguish between real gas leaks and false alarms by considering recent data and historical context. The LSTM's capacity to adjust and recall previous events enables the recognition system to continuously enhance its capabilities, resulting in incremental improvements in performance and accuracy over time. It is numerically demonstrated that the proposed scheme achieves a remarkable degree of accuracy in gas leakage estimation, effectively reducing the potential for accidents and environmental hazards, and substantially enhancing the reliability of hydrogen utilization across various applications. Integrating sensor technology with deep learning, as demonstrated in this study, improves the detection of hydrogen gas. The system model was meticulously implemented in MATLAB, and the simulation results clearly exhibit substantial improvements in the speed and accuracy of hydrogen gas leak detection. Through the utilization of Long Short-Term Memory (LSTM) deep learning, our approach not only enhances leakage prediction but also ensures operational efficiency and a higher level of reliability. Consequently, it offers a fitting solution for the real-time monitoring of hydrogen levels, which represents an important stride toward a more dependable use of this clean energy source [24-25].

2. Problem Statement

There are two main approaches to calculating gas leakage in pipelines, the gas flow is emitted through a hole in the pipe, and in the second case, the diameter of the hole is equal to or larger than the diameter of the pipe, and it is called the destruction of the pipe. We analyze the first case, which is depicted in Figure 1 [26-28].

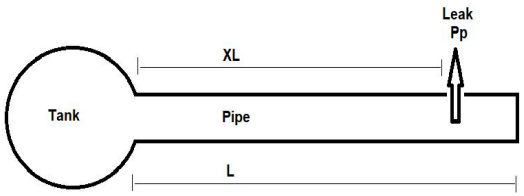

Figure 1- tank, pipeline, and valve

2.1 Hydrogen Gas Leak Behavior

The equations governing the transportation of hydrogen gas in a pipeline, which are derived from the principles of mass and momentum conservation, are provided,

$$\frac{\partial \rho}{\partial \mathrm{t}} + \frac{\partial \rho_u}{\partial x} = 0 \tag{1}$$

$$\frac{\partial \rho_u}{\partial \mathrm{t}} + \frac{\partial (\rho_u{}^2 + \mathrm{P})}{\partial x} + \frac{\mathcal{F}\rho_u|\mathcal{u}|}{2\mathcal{D}} + \rho_{\mathrm{g}} \sin(\theta) = 0 \tag{2}$$

$$U = \frac{\mathrm{Q}}{\mathrm{A}}, \mathrm{A} = \frac{\mathrm{Q}\pi\mathrm{D}^2}{4} \tag{3}$$

Ua: Gas velocity (4)

Pa: Pressure

D: Diameter

$\mathcal{u}$: Volumetric flow rate

$\mathcal{F}$: Coefficient of friction

g: Gravitational force

θ: Angle between friction force and direction

$$\rho a(0, \mathrm{t}) = \rho_0(\mathrm{t}) \tag{5}$$

$$\mathcal{u}a(0, t) = \mathcal{u}_0(t)$$

ρ_0: density at time t=0

u_0: velocity at time t=0

it is assumed that initial conditions are steady state [29].

$$\frac{p\rho_u}{\partial x}(x,0) = 0 \quad (6)$$

$$\frac{\partial(\rho_u{}^2 + p)}{\partial x}(x,0) + \frac{\mathcal{F}\rho_u|u|}{2\mathcal{D}} + \rho_g \sin(\theta) = 0 \quad (7)$$

The typical gas equation of state is as follows:

$$\mathrm{P} = \rho RTa \quad (8)$$

were,

R: Gas constant, Ta: Temperature (9)

The equation of state for the compressible flow is:

$$\mathrm{P} = C^2\rho \quad (10)$$

The ideal gas relation [30]:

$$R = Cp1 - Cv1 \quad (11)$$

$$Y = \frac{Cp}{Cv}, \quad Cv = \frac{R}{Y-1} \quad (12)$$

were,

$Cv1$: The heat capacity at a constant volume (13)

$Cp1$: Specific heat capacity at CP

R: The gas constant

P: Pressure

Y: The flow process index

2.2 Ultrasonic Sensor Behavior

Due to its low weight, hydrogen gas has a considerably higher velocity than air. This inherent attribute allows for the potential measurement of hydrogen concentration in the surrounding atmosphere by evaluating changes in the speed of sound caused by hydrogen leakage [31]. The predominant method utilized in these sensors entails detecting ultrasonic waves and subsequently determining their distance. By utilizing a time-of-flight sound detector between two probes, this sensor can achieve a remarkably short detection time of less than 0.1 ms. Therefore, this method provides practicality in quickly detecting hydrogen leakage, enabling fast and efficient response actions. A transmitter and a receiver are the two components that make up ultrasonic sensors. The piezoelectric crystals that are used by the transmitter are responsible for the emission of sound waves, and the receiver is responsible for picking up on the waves that are entering and leaving the target [32-33]. By calculating the amount of time, it takes for sound to travel from the transmitter to the receiver, the sensor is able to ascertain the distance that exists between itself and the object being identified.

Through the use of the following formula, the computation is determined:

$$D = \frac{2TC}{4} \quad (14)$$

where D represents the distance, T represents the time, and C represents the speed of sound, which is about 343 meters per second [34]. Ultrasonic sensors possess the capability to gauge distance and identify the existence of an object or gas without the need for direct physical contact. Figure 2 displays the measurement of the time it takes for ultrasonic waves to travel.

On the other hand, the velocity of the ultrasonic sensor is affected by external environmental factors such as temperature, humidity, and ambient noise within the frequency range. The measuring range diminishes with each subsequent rise in temperature. While the speed of measurement may decrease as humidity levels rise, this concern can typically be disregarded. The relationship between temperature and humidity attenuation is non-linear. The correlation between temperature and sound speed is nearly linear, as depicted in Figure 3.

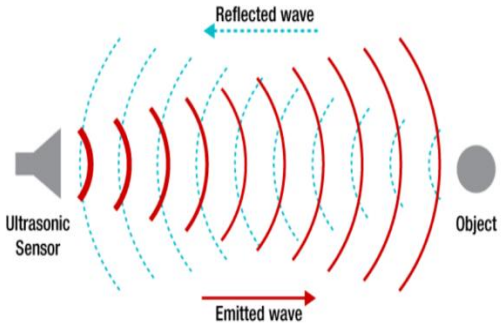

Figure 2- Ultrasonic Time-of-Flight Measurement

When contrasted with the speed with which the gas is expelled from the hole that is leaking, the amount of energy that is lost as a result of the temperature shift that occurs between the surrounding environment and the gas that has fled is often fairly little. This is due to the fact that the speed at which temperature is transferred is very sluggish. As an additional point of interest, the flow of gas that is seen flowing out of the leaking hole is the flow that is believed to be isentropic.

As a result, the formula for the Reynolds number for the gas leak is as follows:

$$Re = \frac{utd}{\frac{\mu}{\rho c}} \quad (15)$$

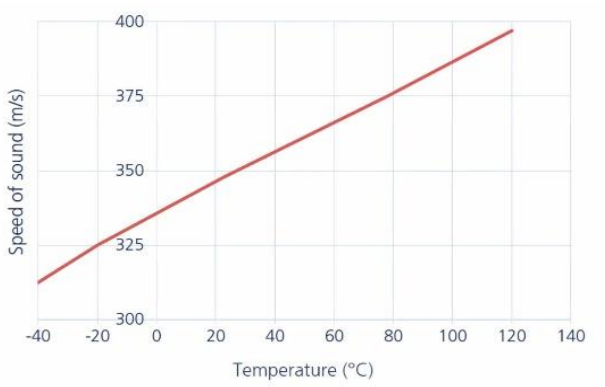

Figure 3- Relationship between temperature and speed of sound

Within this context, the symbol μ is used to denote the viscosity of the gas at the precise moment that it is discharged from the leak. The air's viscosity at a temperature of twenty degrees Celsius and a pressure of 0.101325 MPa is approximately 11.81 × 10^-6 kPa·s. Last but not least, the diameter of the leak hole is denoted by the letter d. On the other hand, the correlation between the intensity of sound and the pressure of sound, and sound power is as follows:

$$I = \frac{W}{S} = \frac{P^2}{\rho c} \quad (16)$$

I represents the intensity of the sound, W represents the power of the sound, S represents the area of the acoustic wavefront, P is sound pressure, ρ is density of the medium through which the sound travels, and c is the speed of sound.

In most cases, the pores in vessels or pipelines that enable leaks to occur are exceedingly minute, with pore diameters often measuring 0.1 mm or even less. There is a large difference between the size of the leak hole and the wavelength range of the waves that are generated by leakage, which falls between 1000 mm and 10 mm. The velocity and frequency of sound waves are known to stay unchanged as they move through a medium that is uniform, whereas the wavelength of the sound waves remains unchanged [35]. As a result, the region in which the waves are generated may be considered a source of sound points, and the waves themselves can be considered to be spherical waves. That being said, the region of the acoustic wavefront is:

$$S = 4\pi r^2 \quad (17)$$

The equation of sound pressure may be found by combining Equations (16) and (17), which are as follows:

$$P = PCW4\pi r \quad (18)$$

In this equation, S represents the distance between the wavefront and the source of the sound. As can be observed in Equation (14), the distance between the sensor and the source of the sound has an inverse relationship with the sound intensity.

2.3 Optical Sensor Behavior

Hydrogen fuel is the most practical choice when it comes to the storage of chemicals that are derived from fossil fuels. There is a high potential energy density associated with it, and it may be obtained from any location on the planet. The sensors that detect hydrogen need to have properties that go beyond just being "spark-free" in order to monitor concentrations and locate leaks of hydrogen in an effective manner. They demand a high level of sensitivity, a significant amount of stability, and a quick response time. In addition to being essential for the development of a hydrogen economy in the future, high-performance hydrogen sensors are also significant in a variety of other fields, such as the chemical industry, the food industry, medical applications, nuclear reactors, and the control of environmental pollution [36-38]. Nanoengineering has the potential to increase the structure of optical sensors, therefore allowing them to respond to hydrogen gas at a rate of less than three times the speed of light (<3 at 1 mbar H2) while having a high level of accuracy (<5%). It is possible to deduce variations in the refractive index near resonance with the use of the general equation for dispersion of the refractive index at the resonant frequency. This equation is as follows:

$$\Delta \mathcal{n}wa=14\pi 2NicSiW0i-W(W0i-w)2+\gamma 2 \qquad (19)$$

Ni is the gas molecular species density, c is the gas concentration in the atmosphere, S_i is the line intensity, ,$W0_i$ is the resonant frequency of the line, and γ is the Lorentzian half-width at half maximum.

γ symbolizes the cumulative impact of gas self-broadening and atmospheric broadening by the host (air) in the designated air-gas combination [39].

There are a several ways to explain the reflectance of a low-finesse that has a constant length L but a variable (i.e., frequency dependent) RI along its optical path:

$$R_{I=}PRP0=2R[1+\cos(4\pi Lf\ c\pi f\ ] \qquad (20)$$

where P_R /P_0 is relative reflectance, R is reflectance of the interferometer's mirrors, L is the distance between mirrors, f is the optical frequency, f is the speed of light, Furthermore,π(f) denotes the frequency-dependent refractive index of the gas.

From the statement that was just presented, the local peak locations in the relative reflectance of the interferometer may be stated as follows: cThe variable m represents an integer fringe index in the optical frequency domain, the variable f_m represents the optical frequency of the fringe or peak with the index m, and the variable nm represents the refractive index of the gas at the optical frequency. All of these variables are included in this equation. It is possible to rewrite the phrase that was made above as follows:

$$mfm=cm2Lnm \qquad (21)$$

The difference in optical frequency Δfm between nearby peaks, such as fringe periods, may be stated as follows under certain circumstances:

$$\Delta fm=\frac{c}{2l}\left(\frac{m+1}{n_m+1}-\frac{m}{n_m}\right) \qquad (22)$$

2.4 Electromagnetic Sensor Behavior

Today, hydrogen gas is considered as a potential alternative to fossil fuels, however, its inherent high flammability raises safety concerns and necessitates the development of reliable and efficient leak detection systems. One of the promising approaches is the use of electromagnetic sensors, which have several advantages over traditional detection methods [40-41].

-Sensitivity and Accuracy: Electromagnetic sensors exhibit exceptional sensitivity and accuracy in detecting hydrogen gas leaks. These sensors operate by measuring changes in the magnetic field induced by hydrogen gas, allowing for precise and real-time detection. The electromagnetic approach enables detection at concentrations as low as parts per million (ppm), making it ideal for identifying even minuscule leaks. By providing accurate measurements, electromagnetic sensors facilitate early detection.

-Non-invasive and Contactless Operation: One significant advantage of electromagnetic sensors is their non-invasive and contactless nature. Traditional leak detection methods often require direct contact with the gas or physical penetration into the pipeline, which can be time-consuming, intrusive, and hazardous. In contrast, electromagnetic sensors enable remote monitoring, eliminating the need for physical access to the gas source. This feature is particularly advantageous when dealing with inaccessible or hazardous environments, such as confined spaces or high-pressure systems [42].

-Low Maintenance Requirements Other benefits of electromagnetic sensors for hydrogen gas leak detection include minimal maintenance. These sensors are strong, sturdy, and temperature- and humidity-resistant. Their non-intrusive operation reduces physical wear and tear, extending their

lifespan. Electromagnetic sensors don't need consumables or calibration gasses, lowering maintenance expenses. The voltage differential transverse to electron passage in an electric conductor is called the "Hall voltage". The magnetic field is the difference between the current and the perpendicular magnetic field. It is possible to separate the hall effect into two distinct types, namely the ordinary hall effect (OHE) and the exceptional hall effect (EHE), based on the magnetic materials that are the source of the hall effect. In order to take advantage of the advantageous properties that they make available to the manufacturing process, the OHE and EHE concepts are utilized in the production of magnetic sensors [43]. Monitoring the change in voltage is one of the components of the OHE technique. The following is a definition of the sensor responses for oxidizing gas:

$$So=(vg-va)va \tag{23}$$

The hall voltages in air and target gas are represented by v_a and v_g. Remember that this is crucial. When the OHE is the lone factor, the equation specifies the Lorentz force's hall voltage on moving charge carriers. In this scenario, only the OHE is examined.

$$VH=RH\times(I\chi\times BZ)\times d\gamma \tag{24}$$

In light of the fact that the hall resistance of the semiconductor,

$$RH=1e(p-nb2p+nb2) \tag{25}$$

$$b=\mu n1\mu\rho 1 \tag{26}$$

The elements p represent the concentration of electrons and holes, $\mu n1$ and $\mu\rho 1$ represent the mobility of electrons and holes, respectively, and e represents the elemental charge, which is the electron. According to the law of mass action, the concentrations of electrons and holes in a semiconductor material that has not been doped are denoted by the symbol i. Assuming that the electron concentration is normalized,

$$RH=(1X-Xb2)\times eni\times(1X-Xb)2 \tag{27}$$

$$p=ni2n,\ X=nni \tag{28}$$

It is possible to determine the hall co-efficient for the active sensor materials in both the presence and absence of the gases by making use of these relations.

$$VH = RH \times I = \frac{i}{T(R_1B + R_2M)} \tag{29}$$

$$R_1 = OHE\,, R_2 = EHE \tag{30}$$

The components of magnetic induction and magnetization perpendicular are denoted by the letters M, T, and B, respectively. I represents the current, T represents the thickness, and B represents the thickness. On the other hand, R_2 Hall effect coefficient is exceptional [44]. R_1 is the ordinary Hall effect coefficient, which is connected to the Lorentz force that acts on moving charge carriers.

3. Method

In previous research conducted by various individuals and organizations, the detection of hydrogen gas using ultrasonic and optical sensors has been investigated separately. However, the goal of our research is to develop a system that provides higher accuracy and detection capability at low PPM levels. To achieve this goal, we have integrated ultrasonic, optical, and electromagnetic sensors into a more comprehensive system. This integrated approach enhances the accuracy of hydrogen gas detection, minimizes errors, and reduces noise interference. Our system consists of three sensors: ultrasonic, optical, and electromagnetic.

By combining these sensors effectively, we can improve the level of hydrogen gas detection and significantly reduce errors and noise during the detection process. To simulate and evaluate the performance of our system, we utilized Simulink, a software tool provided by MATLAB. Simulink simulation considers various environmental conditions, including factors such as temperature, pressure, humidity, and other relevant parameters.

Afterward, with the assistance of deep learning and LSTM, we significantly improved our system's goal of enhancing the accuracy and reliability of hydrogen gas detection, particularly at low PPM concentrations. This research contributes to the advancement of hydrogen gas detection technology and holds the potential to elevate safety measures in industrial, commercial, and residential environments where hydrogen is utilized. we have incorporated an electromagnetic sensor into our system, which makes the proposed approach even more distinctive due to the following advantages:

-Non-electrical gas detection:

In contrast to a great number of other gas sensors, the electromagnetic sensor that we have in our system does not need any kind of electrical contact in order to detect gases. This feature has the ability to not only simplify the setup process but also eliminate the possible risks that are connected with electrical connections in gas detection applications.

-Fast magnetic response:

In comparison to chemical sensors and other kinds of sensors that are quite comparable, the electromagnetic sensor has a reaction time that is far quicker. Because of this greater responsiveness, it is possible to detect gas concentrations more quickly and to monitor them in real time, both of which may be very important in a wide range of applications.

-Low dependence on the ambient temperature:

The electromagnetic sensor has a tendency to be less dependent on the temperature conditions of the surrounding environment, which is one of the key benefits it offers. Even while working in situations with fluctuating temperatures, this characteristic produces gas detection results that are more dependable and stable than those obtained by other methods.

3.1 Measurable Outputs

In this project, extensive research has been done on sensors, which has analyzed various factors affecting their performance. Based on these studies, each sensor has demonstrated the ability to detect hydrogen gas at specific time intervals, as shown in Figure 4. Among these sensors, the electromagnetic sensor stands out as the most accurate sensor, especially in detecting gas leaks at short distances. In Figure 4, the performance curves of different sensors are shown. Curve 'a' is the performance of the optical sensor, curve 'b' corresponds to the electromagnetic sensor, and curve 'c' belongs to the ultrasonic sensor. A comparison of these curves clearly shows the superior accuracy and performance of the electromagnetic sensor, making it the preferred choice for hydrogen gas detection, especially when dealing with short-range detection scenarios.

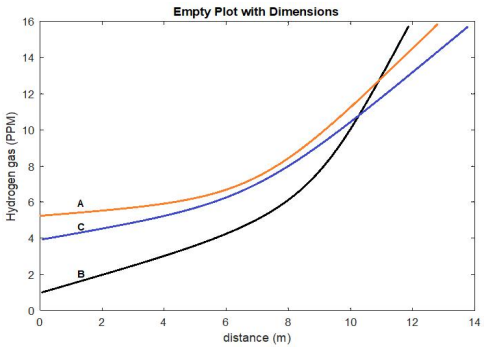

Figure 4- Hydrogen gas detection in ppm by distance

The strengths of each sensor are used, and three distinct kinds of sensors are combined in order to optimize performance and correct any faults that take place. For the purpose of detecting hydrogen gas, we have developed a system that is both comprehensive and efficient. At the same time as the rapid reaction and precision of the electromagnetic sensor play a significant role in maintaining the safety and effectiveness of the gas detection system, the integration of numerous sensors provides an opportunity to improve the reliability and accuracy of the system. Using deep learning and LSTM, we were able to enhance the simulation results that were acquired using MATLAB software for the hydrogen gas detection system. This allowed us to achieve correct results for the detection of hydrogen gas. For the purpose of the MATLAB simulation, we have created an environment that has the following characteristics: every sensor detects hydrogen gas in terms of parts per million (ppm) during the course of twenty-four hours and at intervals of thirty seconds. There is additional consideration given to noise and other issues. Subsequently, we stored these findings in the form of three Excel files, integrated them, and by merging the data of the three sensors, as shown in Figure 5, we generated the final graph of hydrogen gas detection by these three sensors in this period.

Humidity = 50%	Air density = 1.184 kg/m3
Noise = 0.1	Gas concentration = 30 ppm
Gas density = 0.08988 kg/m^3	Gas flow rate = 0.1 m^3/s
Molecular weight of gas = 2.016 g/mol	Distance to hydrogen gas leak = 2.5meters
Actual hydrogen gas leakage = 13 ppm	Gas diffusion coefficient = 0.61e-4 m^2/s

Table 1- shows the simulation conditions

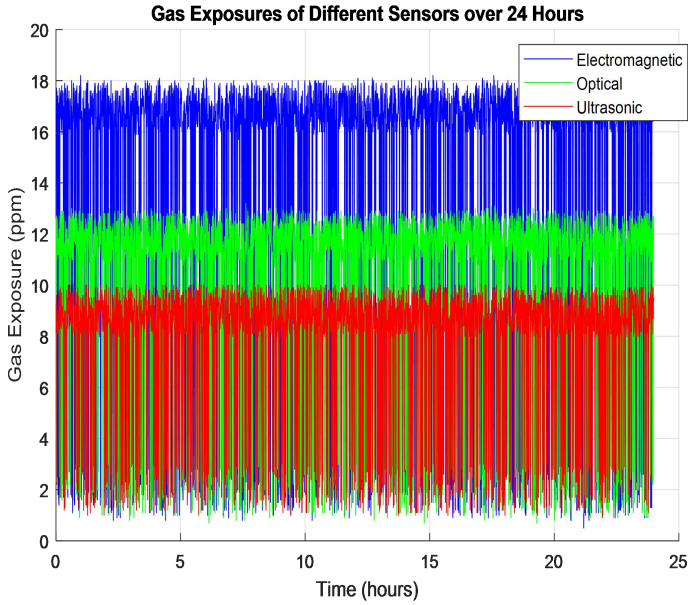

Figure 5- Hydrogen gas detection chart

3.2 Deep Learning, LSTM

Recurrent Neural Networks (RNNs) with Long Short-Term Memory (LSTMs) may find correlations in sequential data over time. You may examine sequential data using LSTMs. They avoid the vanishing gradient problem of traditional RNNs by managing data flow via memory cells and gates. This lets them preserve or remove data as needed. Long short-term memory is used for various things, including time series forecasting. LSTMs have input, forget, and output gates. Information enters the memory cell under the control of the input gate. When data is released from a memory cell, the forget gate regulates it. Data is routed from the long short-term memory (LSTM) to the output by means of the output gate. As a deep learning technique, LSTM constantly uses incoming data to improve the system's prior knowledge. Long Short-Term Memory (LSTM) is the process of training the model to adapt to changing system states as they occur in real time inside this project. The goal of this approach is to add new data without changing the system's current state of knowledge.

A picture of the progression of learning that takes place may be seen in Figure 6. As the figure demonstrates, the learning strategy is the one that is responsible for receiving input and bringing the parameter values of the prediction model up to date. This responsibility is borne by the learning strategy. When a new sort of input is obtained, the model is updated so that it takes into consideration the predictions that were created in the past. This occurs anytime the model receives that new kind of input. Due to the fact that this is the case, the algorithm is able to easily acquire new information and adjust its model in order to include what it has learnt.

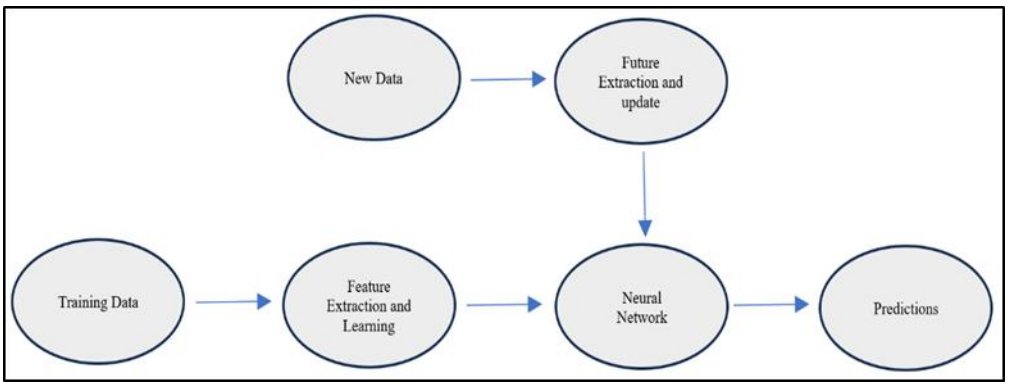

Figure 6- LSTM learning methodology in the project

Within the context of managing extended sequences and ameliorating the constraints associated with conventional Recurrent Neural Networks (RNNs), Long Short-Term Memory (LSTM) networks have gained substantial traction as a widely embraced solution. LSTM networks are purposefully crafted to capture protracted dependencies in sequential data, rendering them exceptionally well-suited for endeavors involving extensive time series or sensor-derived datasets. In the context of this scholarly contribution, we introduce an LSTM-based neural network meticulously tailored for the task of estimating hydrogen gas detection from sensor-generated data. Furthermore, we propose an innovative training paradigm in which the model undergoes

incremental learning through batch processing during runtime, thereby enhancing its adaptability to new and real-time data streams. To help with sensor fusion for attitude estimation, we have developed an Incremental Learning Long Short-Term Memory (LSTM) network, and Figure 7 shows the architectural blueprint for this network. Each of the three sensors contributes their respective measurements as inputs, which are subsequently concatenated to compose an input array. To appraise the prevailing system state, we employ measurements derived from both the present and preceding temporal instances as input features. The instantiated model comprises two discrete strata of LSTM units, wherein a supervised LSTM mechanism is judiciously employed to distill salient features from the input data and culminate in the generation of the requisite output.

During the predictive phase, estimations are computed based on sensor measurements, and at fixed intervals, the model's output rejuvenates to assimilate new insights from the input data, enhancing detection precision. Our research employs a 30-second update interval for recalibrating weights across the temporal sequence. The operational framework and systematic progression of our methodology are elucidated in Figure 8, while Figure 9 comprehensively explains the stages involving attitude estimation and incremental learning.

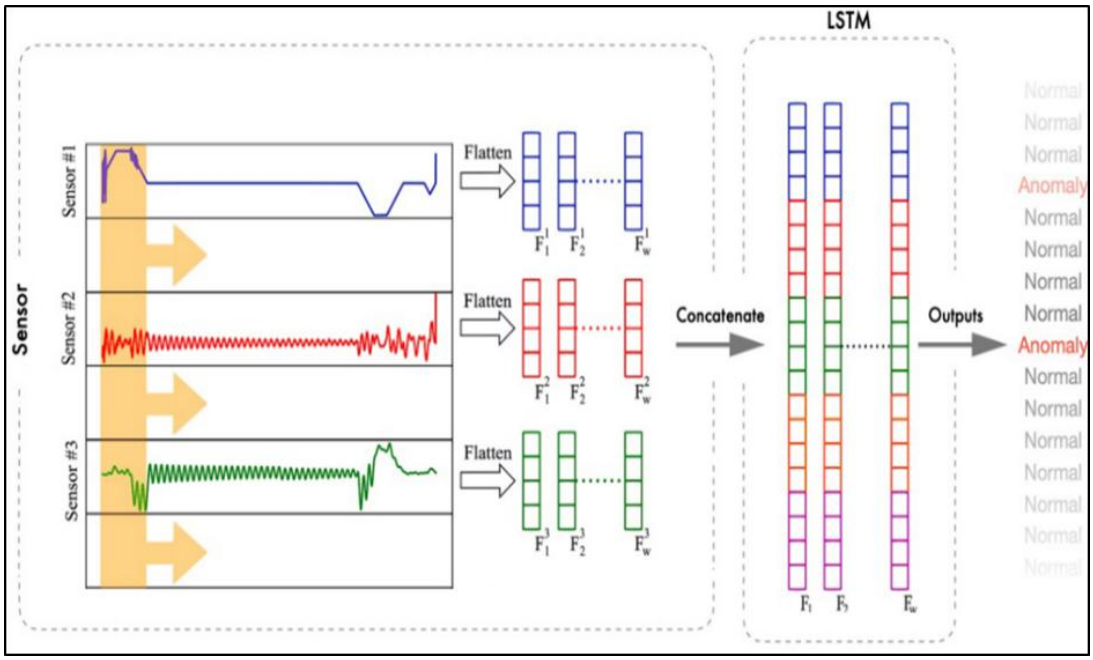

Figure 7- Proposed LSTM based incremental learning framework for attitude estimation

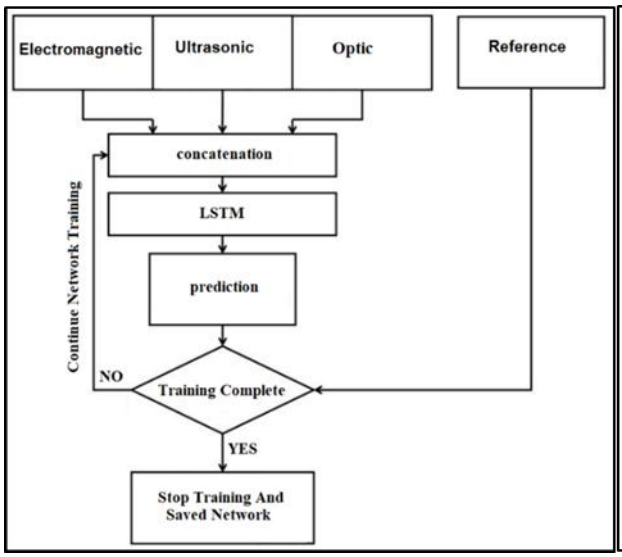

Figure 8- Sensor fusion using LSTM for attitude estimation

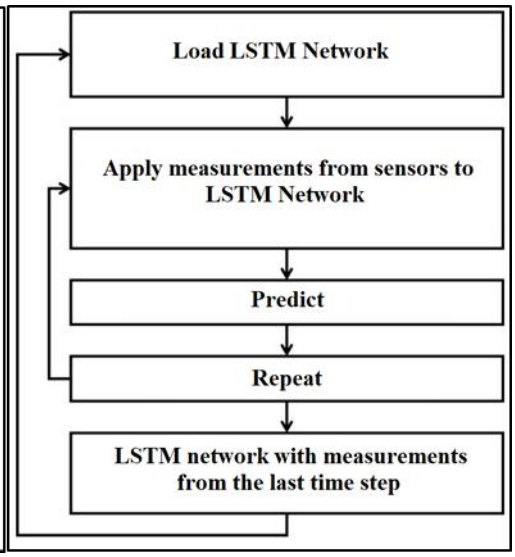

Figure 9- phases of progressive learning and attitude estimation

After assessing the hydrogen gas levels using each sensor, as depicted in Figure 10, it becomes apparent that the resulting data exhibits inherent noise and minor fluctuations. These fluctuations in the sensor measurements have the potential to adversely affect the accuracy of leakage detection within different sections of the system. To overcome this challenge and enhance the precision of our leakage detection system, we've incorporated LSTM (Long Short-Term Memory) neural networks.

The LSTM model serves as a vital component in guiding the system on how to extract more accurate leakage information from the data collected by individual sensors. This integration significantly improves the overall accuracy of our detection process. For a comprehensive overview of the sensor data, we provide Table 2, which documents the detection values recorded by each individual sensor over a one-hour period. These values are presented in their original form, including noise and error, along with the inclusion of all ambient variables.

To consolidate the insights garnered from the three sensors, we've combined the data into a unified dataset and further refined it using LSTM techniques. This data integration approach enhances the robustness and precision of our analysis of sensor measurements, resulting in significantly improved leakage detection capabilities.

TIME	ELECTROMAGNETIC	OPTIC	ULTRASONIC	TIME	ELECTROMAGNETIC	OPTIC	ULTRASONIC
1	13.3	14.6	7	13	1.4	15.5	11.8
2	5	8.8	11.8	14	14.6	14.8	9.8
3	7.5	15.4	11.9	15	13.1	13.9	11.5
4	9	14.3	11.6	16	13.8	14.8	8.9
5	13.2	15.5	11.9	17	14.6	15.7	10.2
6	14.2	14.8	12.1	18	14.4	11	12.4
7	13	14.4	11.8	19	13.8	10.8	13
8	14	14.8	11.5	20	13.5	15.1	11.9
9	13.9	15.1	12.3	21	14.6	15.8	9.8
10	12.9	14	12	22	13	14.5	13
11	13	15.2	12.4	23	14.4	15.8	11.2
12	13.3	15.7	12.1	24	13.8	13	12.2
25	13	13	12.6	43	14.2	15.1	11.8
26	15	6	12.3	44	14.6	14.6	12.4
27	13	8.6	11.5	45	13.9	9.8	11.9
28	14.9	5	12.2	46	1.7	14.1	11
29	13.1	14.3	11.1	47	14.1	15.1	13
30	14.4	13.8	12.5	48	14	15	12.3
31	13.5	9	12.7	49	13.6	14.6	2.3
32	5.9	14.9	11.3	50	2.7	14.4	12.1
33	14.3	11	11.4	51	13.8	15.8	11.1
34	13.6	15	11.8	52	4.8	13.9	11.8
35	14.4	14.8	11.8	53	13.1	15.1	13
36	13.6	15.7	5.8	54	13.6	15.7	8.6
37	2.7	15.5	12.1	55	15	14.7	7.9
38	13.8	6.8	13	56	13.8	15.5	12.9
39	14.8	11.1	11.1	57	14.4	15.1	12.8
40	13.7	14.4	12.1	58	13.4	15.3	9.9
41	13.2	14.1	12.9	59	14.7	15.5	12.9
42	13.3	8.6	12.8	60	14.1	15.5	11.8

Table 2- Detecting the amount of hydrogen gas in ppm

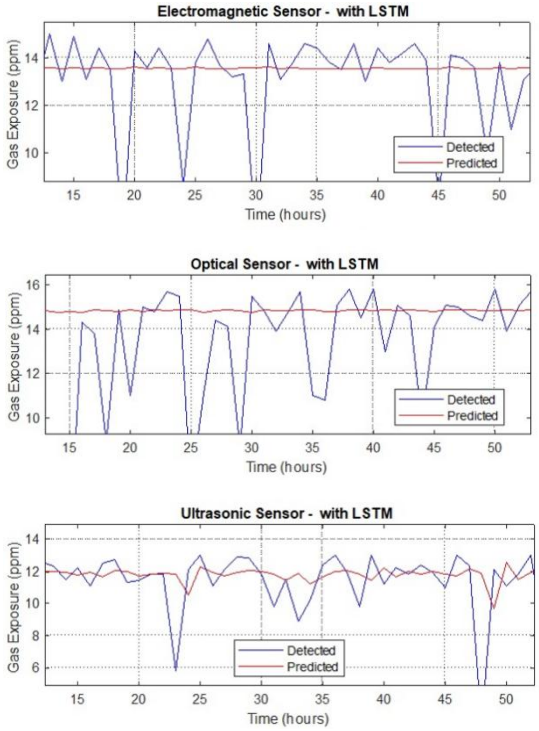

Figure 10- Sensor-detections by LSTM implementation

Utilizing this method, we achieved a highly effective means of discerning precise hydrogen gas leakage values while adeptly filtering out existing noise and errors. The true hydrogen gas leakage level stands at 13 ppm, and our technology consistently detected 13.8 ppm of hydrogen gas at a distance of 2.5 meters from the source, with detailed training specifications provided in Table 3 for reference.

In Figure 11, a visual representation of the training progress for sensor data using LSTM deep learning is presented. This section provides valuable insights into the iterative refinement of our model and includes RMSE (root mean square error) values and loss values measured in iteration units.

These metrics allow for a thorough and accurate evaluation of the model's performance and convergence over time. The substantial progress achieved in hydrogen gas detection owes its success to the integration of ultrasonic, optical, and electromagnetic sensors. Figure 12 illustrates the graph of hydrogen gas values detected by our system, showcasing the combined outputs of these three sensors while effectively eliminating noise disturbances through the implementation of the LSTM model.

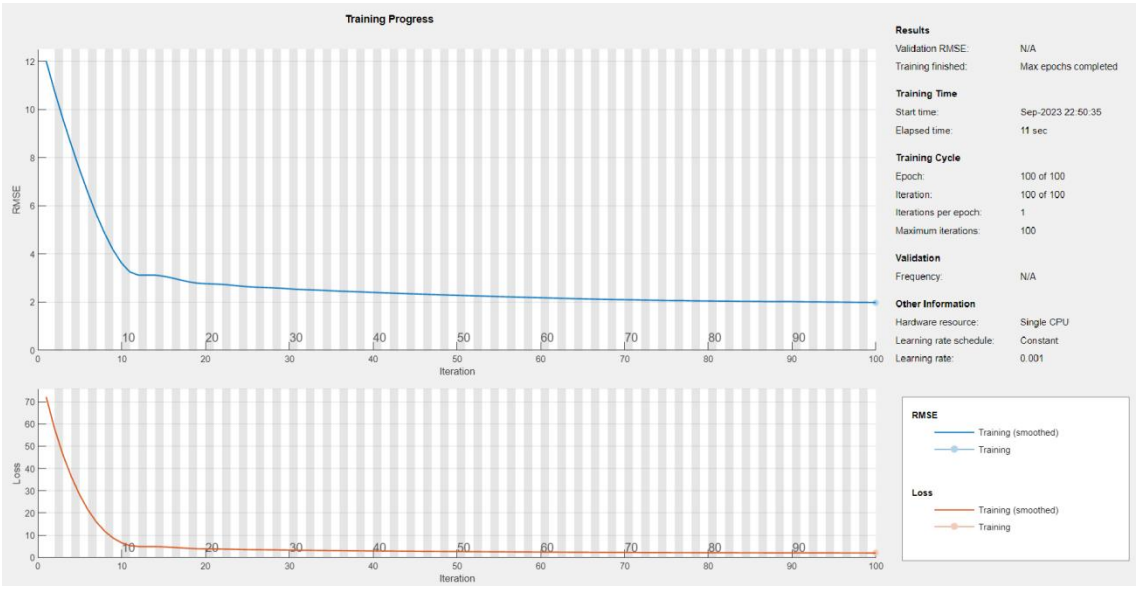

Figure 11- Training Progress

Epoch	Iteration	Time Elapsed(hh:mm:ss)	Mini-batch (RMSE)	Mini-batch (Loss)	Base Learning (Rate)
1	1	00:00:03	14.68	107.7	0.0010
50	50	00:00:25	6.32	20.0	0.0010
100	100	00:00:47	6.24	19.5	0.0010

Table 3-Training table

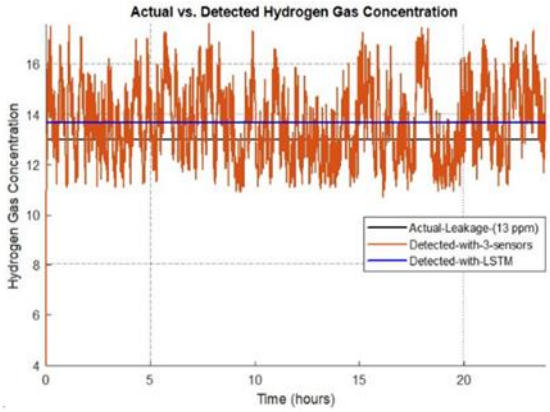

Figure 12- Detection of hydrogen gas from system data using LSTM

4. Conclusions

This research aims to improve the detection of hydrogen gas leaks by utilizing a comprehensive multi-sensor design methodology that incorporates electromagnetic, ultrasonic, and optical sensors. Moreover, it utilizes sophisticated deep learning techniques, specifically the Long Short-Term Memory (LSTM) approach. The system model was implemented utilizing MATLAB, and the resulting simulation outcomes exhibit substantial potential in accelerating the detection of hydrogen gas leaks. By utilizing LSTM deep learning training on the simulated data, we successfully detected a hydrogen gas leak with a concentration of 13.8 parts per million (ppm).

Our future research aims to perform experiments in real industrial environments to evaluate the efficacy of detection in intricate network structures and a wider range of work situations. By doing so, we will be able to authenticate and enhance our methodology in practical situations.

5. Funding and Data Availability

All the research data is available to share with the reader. Please contact the first author to get access to the data and simulation files. This work was funded by a Lamar University internal grant without any conflict of interest for the authors.

References:

[1] CevahirTarhan, Mehmet Ali Çil, A study on hydrogen, the clean energy of the future: Hydrogen storage methods, Journal of Energy Storage, Volume 40, August 2021, 102676

[2] Iain Staffell ORCID, Daniel Scamman, Anthony Velazquez Abad, Paul Balcombe, Paul E. Dodds, Paul Ekins, Nilay Shah and Kate R. Ward, The role of hydrogen and fuel cells in the global energy system, DOI: 10.1039/C8EE01157E (Review Article) Energy Environ. Sci., 2019, 12, 463-491

[3] Ahmed I. Osman, Neha Mehta, Ahmed M. Elgarahy, Mahmoud Hefny, Amer Al-Hinai, Ala'a H. Al-Muhtaseb& David W. Rooney, Hydrogen production, storage, utilisation and environmental impacts: a review, Published: 06 October 2021, volume 20, pages153–188 (2022)

[4] Jiawei Tian, Hongchuan Jiang, Xinwu Deng, Luying Zhang, Jianfeng Zhang, Xiaohui Zhao, Wanli Zhang, Zero drift suppression for PdNinano-film hydrogen sensor by vacuum annealing, Volume 45, Issue 28, 21 May 2020, Pages 14594-14601

[5] Shivani Dhall, B.R. Mehta, Room temperature hydrogen gas sensor using candle carbon soot, Volume 45, Issue 29, 26 May 2020, Pages 14997-15002

[6] Sheng Mao, Han Zhou, Shuanghong Wu, Junjie Yang, Zhongyuan Li, Xiongbang Wei, Xiangru Wang, Zhiyong Wang, Jie Li, High performance hydrogen sensor based on Pd/TiO2 composite film, Volume 43, Issue 50, 13 December 2018, Pages 22727-22732

[7] Salvatore Gianluca Leonardi, Anna Bonavita, Nicola Donato, Giovanni Neri, Development of a hydrogen dual sensor for fuel cell applications, Volume 43, Issue 26, 28 June 2018, Pages 11896-11902

[8] Fan Zhang, Pengcheng Zhao, Meng Niu, Jon Maddy, The survey of key technologies in hydrogen energy storage, Volume 41, Issue 33, 7 September 2016, Pages 14535-14552

[9] A.V. Kroll, V.Smorchkov, A.Y. Nazarenko, Electrochemical sensors for hydrogen and hydrogen sulfide determination, Volume 21, Issue 2, August 1994, Pages 97-100

[10] Maria Moßhammer, Michael Kühl, Klaus Koren, Possibilities and Challenges for Quantitative Optical Sensing of Hydrogen Peroxide, Chemosensors 2017, 5(4), 28

[11] Wei Chen , Shu Cai , Qiong-Qiong Ren , Wei Wen and Yuan-Di Zhao, Recent advances in electrochemical sensing for hydrogen peroxide: a review, DOI: 10.1039/C1AN15738H Analyst, 2012, 137, 49-58

[12] T. Watanabe, S. Okazaki, H. Nakagawa, K. Murata, K. Fukud, A fiber-optic hydrogen gas sensor with low propagation loss, Volume 145, Issue 2, 19 March 2010, Pages 781-787

[13] J.Z. Sasiadek, Sensor fusion, Volume 26, Issue 2, 2002, Pages 203-228

[14] Ren C. Luo; Chih Chia Chang; Chun Chi Lai, Multisensor Fusion and Integration: Theories, Applications, and its Perspectives, 29 August 2011, DOI: 10.1109/JSEN.2011.2166383

[15] T.D. Larsen; K.L. Hansen; N.A. Andersen; Ole Ravn, Design of Kalman filters for mobile robots; evaluation of the kinematic and odometric approach, 06 August 2002, DOI: 10.1109/CCA.1999.801027

[16] Peter Willett; Alan Marrs; Francesco Palmieri; Stefano Marano, Practical fusion of quantized measurements via particle filtering, January 2008, DOI: 10.1109/TAES.2008.4516986.

[17] Michael Aeberhard, Nico Kaempchen, High-Level Sensor Data Fusion Architecture for Vehicle Surround Environment Perception

[18] Parag Narkhed, RaheeWalambe, Shruti Mandaokar, Pulkit Chandel, Ketan Kotecha and George Ghinea, Gas Detection and Identification Using Multimodal Artificial Intelligence Based Sensor Fusion, 9 January 2021

[19] Sören Dierks; Andreas Kroll, Quantification of methane gas leakages using remote sensing and sensor data fusion, 12 April 2017, DOI: 10.1109/SAS.2017.7894047

[20] N. Kaempchen; M. Buehler; K. Dietmayer, Feature-level fusion for free-form object tracking using laserscanner and video, September 2005, DOI: 10.1109/IVS.2005.1505145

[21] Parag Narkhede, RaheeWalambe, Shashi Poddar, Ketan Kotecha, Incremental learning of LSTM framework for sensor fusion in attitude estimation, DOI: 10.7717/peerj-cs.662

[22] Alex Sherstinsky, Fundamentals of Recurrent Neural Network (RNN) and Long Short-Term Memory (LSTM) network, Volume 404, March 2020, 132306

[23] Andrew Pulver; SiweiLyu, LSTM with working memory, July 2017, DOI: 10.1109/IJCNN.2017.7965940

[24] Zhifei Wu, Tekuai Li, Yuxia Xiang, Mengfan He, High-pressure under-expanded hydrogen leakage model considering gas-wall friction loss, 23 March 2022, Citations: 2

[25] Selgin AL, Çağatay YAMÇIÇIER, Mechanical and Structural Evaluation of LiSrH3 Perovskite Hydride for Solid State Hydrogen Storage Purposes, 2022, , 799 - 804, 31.08.2022

[26] Jingxuan Liu, Lin Teng, Bin Liu, Peng Han, Weidong Li, Analysis of Hydrogen Gas Injection at Various Compositions in an Existing Natural Gas Pipeline, Energy Res, 16 July 2021, Hydrogen Storage and Production Volume 9 – 2021

[27] Sarkhosh S. Chaharborj, Zuhaila Ismail, Norsarahaida Amin, Detecting Optimal Leak Locations Using Homotopy Analysis Method for Isothermal Hydrogen-Natural Gas Mixture in an Inclined Pipeline, October 2020, 12(11), 1769

[28] Bin AiBin, AiYujing Sun, Yiping Zhao, Plasmonic Hydrogen Sensors, DOI: 10.1002/smll.202107882

[29] Jie Zhang, Controlling the pressure of hydrogen-natural gas mixture in an inclined pipeline, 2020; 15(2): e0228955, 2020 Feb 27

[30] WonjunSeo, SeokyeonIm, and Geesoo Lee, Characteristics of the Received Signal of an Ultrasonic Sensor Installed in a Chamber with Micro-Leakage, 24 Nov 2021

[31] Xue-Yu Zhang, Ren-Hao Ma, Ling-Sheng Li, Li Fan, Yue-Tao Yang & Shu-Yi Zhang, A room-temperature ultrasonic hydrogen sensor based on a sensitive layer of reduced graphene oxide, Scientific Reports volume 11, 2021

[32] D. Marioli; C. Narduzzi; C. Offelli; D. Petri; E. Sardini; A. Taroni, Digital time-of-flight measurement for ultrasonic sensors, Page(s): 93 – 97, Date of Publication: February 1992, Accession Number: 4170844

[33] Tao Wang, Xiaoran Wang, and Mingyu Hong, Gas Leak Location Detection Based on Data Fusion with Time Difference of Arrival and Energy Decay Using an Ultrasonic Sensor Array, 2018, 18(9), 2985

[34] Markandey M. Tripathi a, Kemal E. Eseller b, Fang-Yu Yueh a, Jagdish P. Singh a, An optical sensor for multi-species impurity monitoring in hydrogen fuel, Volumes 171–172, August–September 2012, Pages 416-422

[35] Hoang Mai Luong, Tu Anh Ngo, Minh Pham, Ultra-fast and sensitive Magneto-Optical Hydrogen Sensors Using a Magnetic Nano-cap Array, DOI: 10.1016/j.nanoen.2023.108332

[36] Matej Njegovec and Denis Donlagi, A Fiber-Optic Gas Sensor, and Method for the Measurement of Refractive Index Dispersion in NIR, Sensors 2020, 20(13), 3717; 11 June 2020

[37] M.R Barzegaran, M. Mirzaie, A. Barzegari, A. Shayegani Akmal4, Determining Sensitive test Configuration of Power Transformers for FRA Measurement using New Approach in Finite Element Analysis

[38] Francisco Javier Ferrández-Pastor, Juan Manuel García-Chamizo and Mario Nieto-Hidalgo, Microstrip Sensors Developing, Sensors 2017, 17(7), 1650;20 June 2017

[39] Matej Njegovec, Denis Donlagic, A Fiber-Optic Gas Sensor and Method for the Measurement of Refractive Index Dispersion in NIR, Sensors 2020, 20(13), 3717

[39] Hoang Mai Luong, Minh Thien Pham, Tyler Guin, Richa Pokharel Madhogaria, Manh-Huong Phan, George Keefe Larsen &Tho Duc Nguyen, Sub-second and ppm-level optical sensing of hydrogen using templated control of nano-hydride geometry and composition, April 2021, 2414 (2021)

[40] Matej Njegovec, and Denis Donlagic, A Fiber-Optic Gas Sensor and Method for the

Measurement of Refractive Index Dispersion in NIR, 2 July 2020

[41] Pedram Asef1, Ramon B. Perpina, M. Reza Barzegaran, Andrew Lapthorn, and Daniela Mewes, Load Identification of Different Halbach-Array Topologies on Permanent Magnet Synchronous Generators Using the Coupled Field-Circuit FE Methodology, 2021 IEEE Power and Energy Conference at Illinois (PECI)

[42] Pratik Shinde, Chandra Sekhar Rout, Magnetic Gas Sensing: Working Principles and Recent Developments, DOI: 10.1039/D0NA00826E

[43] Satyendra K. Mishra, Sandeep N. Tripathi, Veena Choudhary, Banshi D. Gupta, SPR based fibre optic ammonia gas sensor utilizing nanocomposite film of PMMA/reduced graphene oxide prepared by in situ polymerization, Volume 199, August 2014, Pages 190-200

[44] Jochen Krücker, Sheng Xu, Neil Glossop PhD, Anand Viswanathan, JörnBorgert, Heinrich Schulz, Bradford J.wood, Electromagnetic Tracking for Thermal Ablation and Biopsy Guidance: Clinical Evaluation of Spatial Accuracy, Volume 18, Issue 9, September 2007, Pages 1141-1150. Issue 9, September 2007, Pages 114